Surface Science 603 (2009) 1041–1045

Contents lists available at ScienceDirect

Surface Science

journal homepage: www.elsevier.com/locate/susc

Growth and sacrificial oxidation of transition metal nanolayers

Tim Tsarfati [a,*], Erwin Zoethout [a], Robbert van de Kruijs [a], Fred Bijkerk [a,b]

[a] FOM Institute for Plasma Physics Rijnhuizen, Edisonbaan 14, 3430 BE Nieuwegein, The Netherlands
[b] MESA+ Institute for Nanotechnology, University of Twente, Enschede, The Netherlands

ARTICLE INFO

Article history:
Received 22 December 2008
Accepted for publication 18 February 2009
Available online 25 February 2009

Keywords:
d-Metals
Islanding
Sacrificial oxidation
ARPES
Multilayers

ABSTRACT

Growth and oxidation of Au, Pt, Pd, Rh, Cu, Ru, Ni and Co layers of 0.3–4.3 nm thickness on Mo have been investigated with ARPES and AFM. Co and Ni layers oxidize while the Mo remains metallic. For nobler metals, the on top O and oxidation state of subsurface Mo increase, suggesting sacrificial e^- donation by Mo. Au and Cu, in spite of their significantly lower surface free energy, grow in islands on Mo and actually promote Mo oxidation. Applications of the sacrificial oxidation in nanometer thin layers exist in a range of nanoscopic devices, such as nano-electronics and protection of e.g. multilayer X-ray optics for astronomy, medicine and lithography.

© 2009 Elsevier B.V. All rights reserved.

1. Introduction

In d-metal on d-metal layer growth, the d-band configuration and surface free energy difference are of important influence. Electrons may be exchanged to achieve an energetically more favorable half filled d-band with only spin up electrons. Segregation or islanding can occur to minimize surface dangling bonds or contact area. We will consider potentially stable systems where Mo, with an approximately half filled d-band and high surface free energy, forms the substrate layer for on top nanolayer growth of d-metals with a range of surface free energies and oxidation enthalpies.

Surface nanolayers that protect the Mo from oxidation can also have applications in Mo/Si multilayer reflective optics for next generation extreme UV lithography (EUVL). The EUV radiation penetrates and reflects from the top 50 Mo/Si periods, the effective maximum. The reflection from each interface contributes to in-phase EUV reflection, adding up to more than 70%. During EUV exposure in a lithography tool vacuum environment, background C_xH_y and H_2O gases can adsorb and dissociate on the mirror surface. Subsequent carbon contamination and oxidation of the multilayer surface reduce mirror reflectance. Although, the adsorption of volatile C_xH_y species and subsequent carbon contamination can be controlled by extensive outgassing of the vacuum system and cleaning of the mirror surface [1,2], oxidation is generally considered irreversible. To protect the multilayer mirror against oxidation, a thin protective "capping layer" can be applied at the multilayer surface. The aliphatic hydrocarbons that are observed on the caps can partially shield against oxidation but are not explicitly considered in this work as long as they don't appear to be of serious influence. Depending on material choice and cap layer thickness, the theoretical reflectance (R) of a capped 50 period Mo/Si multilayer can vary by tens of percents. We will relate our observations on layer interaction, oxidation, composition, morphology and diffusion to the application of capping layers on Mo/Si multilayers.

2. Experimental details

Si on top Mo and capping layers were grown by e-beam physical vapor deposition (PVD) onto natively oxidized super polished Si substrates in a base pressure of 1×10^{-6} Pa [3]. Growth rates were 0.05 nm/s for Si, 0.04 nm/s for Mo, and 0.01 nm/s for the capping metals. A flux-shaping mask was used to deposit the capping layer with a lateral thickness gradient of 0.3–4.3 nm [4], as determined with quartz crystal oscillator microbalances. The samples were exposed to ambient air for several weeks and subsequently analyzed using angular resolved X-ray photoelectron spectroscopy (ARPES) and scanning Auger microscopy (SAM) in a Thermo Theta Probe with a field emission gun. Simplified, the ARPES measurements between 27° and 64° off normal are modeled to a homogeneous layered system [5] using the factor $e^{\frac{z}{\lambda \cos\theta}}$ from the depth distribution function that relates the detection angle θ via the attenuation length λ [6] to the sampling depth z. In the case of non-homogeneous layer growth, the set of conditions as described by Cumpson [5] is not fulfilled and the modeling can result in estimated layer thickness and in-depth distribution errors of up to several nanometers [7]. XPS depth profiling was performed using 0.5 keV Ar^+.

* Corresponding author.
E-mail address: tsarfati@rijnhuizen.nl (T. Tsarfati).

0039-6028/$ - see front matter © 2009 Elsevier B.V. All rights reserved.
doi:10.1016/j.susc.2009.02.027

An ex-vacuo Schaffer Nanosurf EasyScan 2 high resolution AFM was used to study the lateral material distribution.

3. Layer growth kinetics

The morphology of the capping layer grown on the Mo substrate is physically restrained by the low atom mobility for e-beam PVD that limits deviation from Gaussian (stochastic) layer-by-layer growth [8]. Influence on the morphology subsequently occurs chemically via Young's equation $\Delta H^{\text{total}} = \Delta H^{\text{surface}}_{\text{cap}} + \Delta H^{\text{interface}}_{\text{Mo/cap}} - \Delta H^{\text{surface}}_{\text{Mo}}$ [9,10]. $\Delta H^{\text{total}} \leqslant 0$ generally results in layer-by-layer (Frank–van der Merwe) growth, while $\Delta H^{\text{total}} > 0$ yields island (Volmer–Weber) growth. The relation holds for each individual adlayer, and initial layer-by-layer growth with successive island (Stranski–Krastinov) growth occurs when the substrate-particle affinity is initially strong, but a lattice mismatch between the film and substrate introduces a strain into the growing film [11]. Individual $\Delta H^{\text{surface}}$ and $\Delta H^{\text{interface}}$ values can result in surface free energy driven intermixing even when $\Delta H^{\text{interface}}$ is positive [12]. The segregating material will then agglomerate below the surface to minimize contact area. The Gibbs free energy to form the most stable oxide (ΔG^{form}_0) gives an indication on the suitability of the metal as a protective cap against oxidation. Table 1 shows the $\Delta H^{\text{surface}}$, $\Delta H^{\text{interface}}$, ΔH^{total} and ΔG^{form}_0 for the materials involved [13].

For all metals in Table 1, $\Delta H^{\text{total}} < 0$ when grown onto Mo, favoring layer-by-layer growth. While $\Delta H^{\text{surface}}$ of Au and Cu are lowest of all, the positive $\Delta H^{\text{interface}}$ partially counters wetting of the Mo and favors minimization of the contact area, i.e. Volmer–Weber (island) growth [14]. Mentioned layer thicknesses hereafter are "as-deposited" and refer to equivalents when layer-by-layer growth would have occurred.

4. Results and discussion

As a reference for Mo oxidation and a measure of the protective functionality of a capping layer, a 2.5 nm Mo layer on a 5.0 nm Si layer is deposited without a capping layer. With ARPES we model that approximately 30% of the Mo oxidizes to a MoO_3 film of ~0.6 nm thickness under ambient conditions (Fig. 1). Oxidation accelerates under EUV exposure in lithography tool vacuum due to H_2O dissociation by secondary electrons [1].

The as-deposited oxidation state of uncapped Mo is now compared to the case when a Au capping layer is applied (Fig. 2). As pointed out in the previous section, layer-by-layer and island growth compete while Au intermixture or compound formation with Mo is certainly not expected.

Fig. 2 shows that for Au layers up to 1.5 nm thick, a constant 40% of Mo is oxidized to MoO_3, while the Au does not oxidize. Mo oxidation increases to almost 80% after several months in ambient environment [15]. Modeling of ARPES and XPS depth profiling measurements both indicate layer intermixture, showing

Table 1
$\Delta H^{\text{surface}}$, $\Delta H^{\text{interface}}$ with Mo, ΔH^{total} with Mo, and ΔG^{form}_0 at 298 K in kJ/mole of the respective metals.

	$\Delta H^{\text{surface}}$	$\Delta H^{\text{interface}}$	ΔH^{total}	ΔG^{form}_0
Mo	188			−167
Co	127	−18	−79	−112
Ni	121	−27	−94	−106
Ru	174	−56	−70	−84
Cu	95	67	−26	−64
Rh	155	−59	−92	−60
Pd	124	−59	−123	−41
Pt	152	−114	−150	
Au	99	14	−5	15

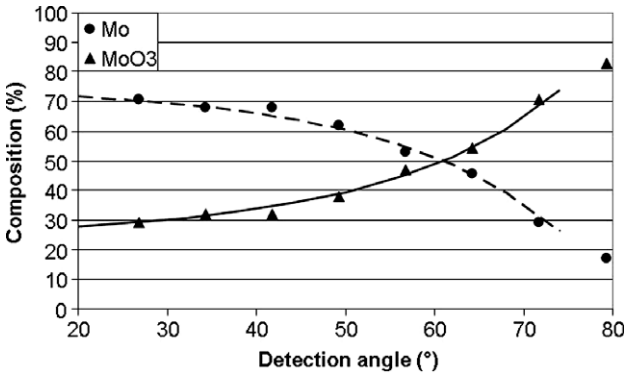


Fig. 1. Modeling of the ARPES results indicates that bare Mo oxidizes to a ~0.6 nm thick MoO_3 layer at the surface in ambient conditions.

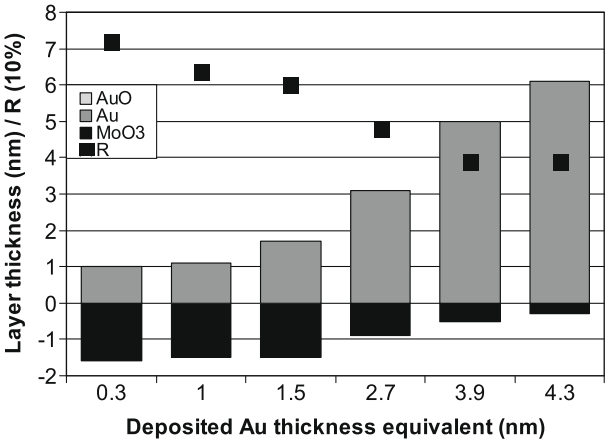


Fig. 2. Modeled ARPES results on the Au cap, with 0 nm defined as the original Au-on-Mo interface. In the positive direction extends the cap adlayer, in the negative direction oxidation of the Mo substrate layer. The calculated reflectance R for a capped 50 period multilayer is also shown.

equivalent amounts of Au and MoO_3 in the top few nm's, and a region of increased MoO_3 to elemental Mo concentration below. It is remarkable that Mo oxidation is actually increased and relatively constant up to 1.5 nm Au. Au islanding or intermixture might expose Mo for oxidation and increase the electron escape depth, causing overestimation in layer thickness modeled with ARPES. With SAM we observe dots of oxygen and a somewhat irregular distribution of Au. Verification of suspected inhomogeneous layer growth is performed with AFM on the 4 nm thick Au capping layer, as shown in Fig. 3.

AFM reveals surface roughness of 3.06 nm (RMS) and a peak-to-valley height of 18.7 nm, a value much larger than the as-deposited Au layer thickness. The difference is most probably explained by grain boundaries, in addition to the agglomeration in islands of typically 100 nm in diameter that we observe in Fig. 3, acknowledging island growth. The activation barrier for interface formation of Au with Mo apparently hinders layer-by-layer growth and protective functionally of Au capping layers.

The next noblest metal, Pt, has the most negative $\Delta H^{\text{interface}}$ with Mo of all metals investigated, favoring intermixture instead of island growth. A range of Pt capping layer thicknesses was characterized with ARPES (Fig. 4).

For a Pt capping layer of 0.3 nm thickness, approximately 70% of the Mo appears oxidized to MoO_3, even more than in the case of Au. When the Pt capping layers thickness is 1.0 nm, about 25% of the Mo is oxidized to MoO_3, for 1.5 nm Pt this is reduced to 10%.

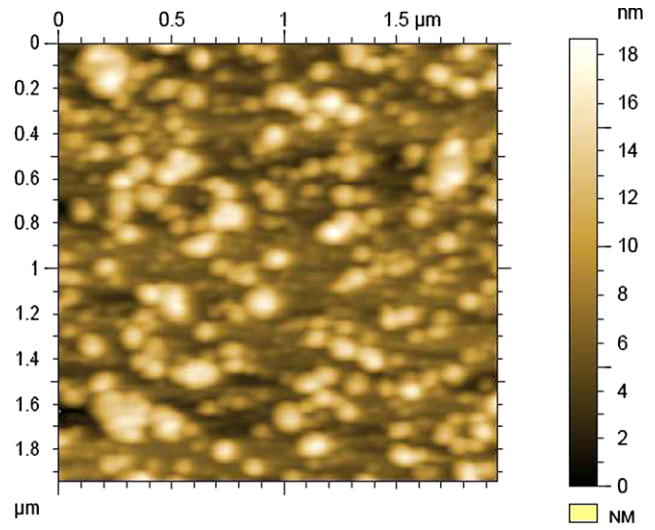


Fig. 3. AFM on a 4 nm thick Au capping layer shows a significant roughness with a lateral structure that suggests Volmer–Weber growth.

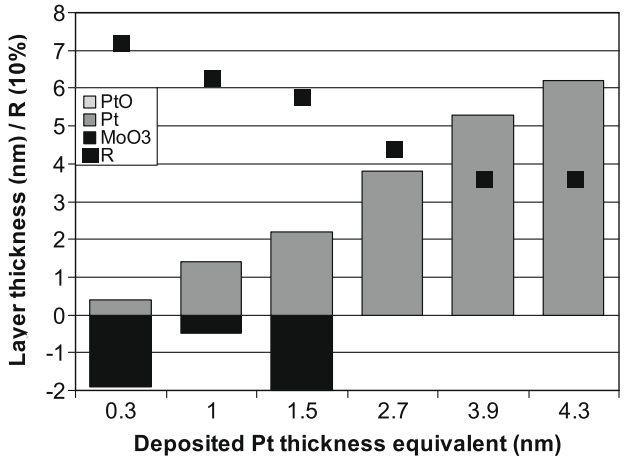


Fig. 4. Modeled ARPES results on the Pt cap, showing subsurface Mo oxidation and layer intermixture.

Modeling of the ARPES measurements suggests significantly thicker Pt layers than were deposited and complete intermixture with abundant MoO_3 for up to 1.5 nm thick Pt layers. The observation by Jeon et al. [16] that Na provides additional oxidation sites in the Ge surface might also apply for the Pt–Mo interlayer. For Pt layers thicker than 1.5 nm, no Mo oxidation and no Mo at grazing detection angles are observed in ARPES, indicating the Pt layer is now closed. XPS depth profiling reveals a Pt/Mo/Si layered structure. The roughness of an as-deposited 4 nm thick Pt capping layer is below the AFM measurement accuracy, suggesting that no islanding indeed occurs.

Pd has a moderately negative $\Delta H^{\text{interface}}$ with Mo, and is expected to grow layer-by-layer with less intermixing compared to Pt on Mo. Fig. 5 shows the surface state as determined with ARPES for the different Pd layer thicknesses.

When a 0.3 nm thick Pd capping layer is applied on Mo, ~85% of the Mo oxidizes. With a 1.0 nm thick Pd layer, this is ~50%, still more than bare Mo. The Pd does not yet appear closed and surface MoO_3 is visible. A 1.5 nm thick Pd capping layer limits Mo oxidation to ~30%. XPS depth profiling reveals that only moderate intermixture occurs. For thicker Pd layers, traces of MoO_3 are visible for all but the most grazing detection angles. The Pd layer appears to

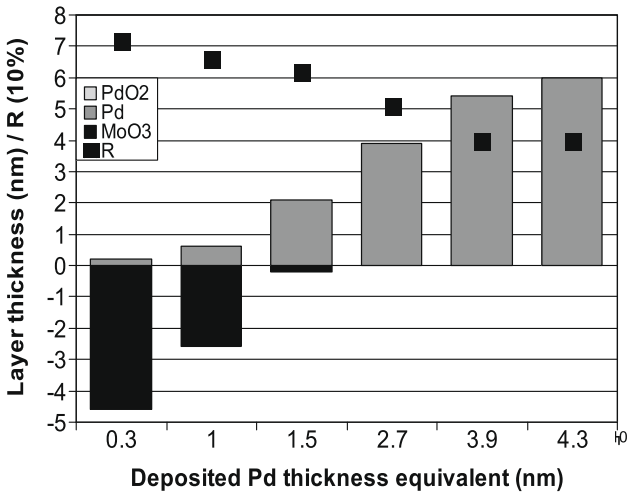


Fig. 5. Modeled ARPES results on the Pd cap, revealing more subsurface Mo oxidation than under Pd.

form a closed layer at the surface in these cases. Traces of PdO are observed near the surface over the complete range of layer thicknesses. The observation that Pd promotes Mo oxidation even more than Pt is not readily fully attributed to creation of extra oxidation sites in the Pd–Mo interlayer, since it's both theoretically and experimentally established to be thinner. We propose here that e^- donation from Mo to the nobler Pd might occur, similar to the extensively studied Pd–H system [17]. In effect, Mo would function as a sacrificial metal and increase its oxidation state.

Having the same $\Delta H^{\text{interface}}$ with Mo as Pd, Rh also is expected to grow layer-by-layer. XPS depth profiling studies have shown that diffusion through the Mo and underlying Si layer and agglomeration at the Si-on-Mo interface prominently occur in the case of Rh [18]. Fig. 6 shows the modeled ARPES results for the characterized Rh layer thicknesses.

A 0.3 nm thick Rh layer yields ~70% Mo oxidization to surface MoO_3, again more than for uncapped Mo. A 1.0 nm thick Rh layer limits Mo oxidation to less than 10%, while thicker Rh layers stop it altogether. A ~0.3 nm thick Rh_2O_3 and on top CO film is formed on the Rh caps that appear significantly thicker in ARPES.

Cu deposition on Mo involves similar considerations as discussed for Au on Mo. The highly positive $\Delta H^{\text{interface}}$ obstructs

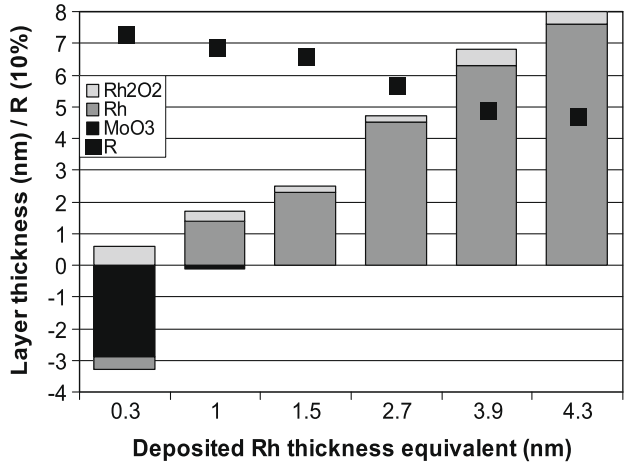


Fig. 6. Modeled ARPES results for the Rh cap, suggesting major layer expansion.

layer-by-layer growth more than Au growth on Mo, but this growth mode is still predicted by Young's law, due to the low $\Delta H^{surface}$ of Cu. A range of Cu capping layer thicknesses was characterized with ARPES (Fig. 7).

With a Cu capping layer, we observe Mo oxidation over the complete layer thickness range as in the case of Au, although the Cu layer thickness is of more influence on the degree of Mo oxidation. For 0.3 nm Cu, about 50% of the Mo is oxidized to MoO_3, for 1.0 nm Cu this is ~35%. With thicker Cu layers, some 20% of the Mo is oxidized. We observe significant amounts of CuO near the surface with both ARPES and XPS depth profiling; in the thickest layers, a CuO film up to 0.7 nm is present. The CuO appears to effectively cover the Mo already for the thinnest Cu layers, albeit not protecting it against oxidation. To study the layer homogeneity, AFM is performed on a 4 nm thick Cu layer, as shown in Fig. 8.

AFM shows a surface roughness of 0.35 nm (RMS) and a peak-to-valley height of 3.1 nm for an as-deposited 4 nm thick Cu capping layer. The lateral resolution of SAM is insufficient to reveal whether chemical inhomogeneity is present at the surface. The observations provide no certainty whether island growth occurs. If so, it is less pronounced than for Au on Mo. This is remarkable, since Au is kinetically less likely to grow in islands on Mo than Cu is. Possibly, Cu oxidation lowers the $\Delta H^{interface}$ with Mo, shifting the balance.

Ru is the material that is generally used as capping material for EUV multilayer mirrors [19]. Due to its moderate optical absorption of EUV, R is considerably higher for multilayers capped with Ru than with any other metal of similar thickness discussed here. Table 1 shows that the $\Delta H^{interface}$ with Mo is similar to that of Pd and Rh. The $\Delta H^{surface}$ is per unit area slightly higher than that of Mo. Ru was also found to diffuse and agglomerate at the Si-on-Mo interface [18]. This might allow for subsequent Mo oxidation, but ARPES reveals that this is not the case, as shown in Fig. 9.

A 0.3 nm thick Ru layer allows Mo to oxidize for about 40% to MoO_3, for 1.0 nm Ru and more, no Mo oxidation occurs under ambient conditions, nor do we identify any Ru oxidation, although the material is less noble than the above mentioned materials. We attribute this to the higher catalytic activity of Ru to dissociate and physisorb C species [1,15]. C is difficult to identify on Ru due to peak overlap in XPS, but it can protect against oxidation of the Ru [20,21]. Also the Ru appears significantly thicker in ARPES, possibly due to the observed diffusion.

Kinetics especially favor Ni and Co layer-by-layer growth, given their low $\Delta H^{surface}$ and moderately negative $\Delta H^{interface}$ with Mo, as is shown in Table 1. Ni and Co yield a lower R and are more susceptible to oxidation than earlier discussed metals, but could still protect against Mo oxidation. Fig. 10 shows the ARPES characterization of the Ni caps.

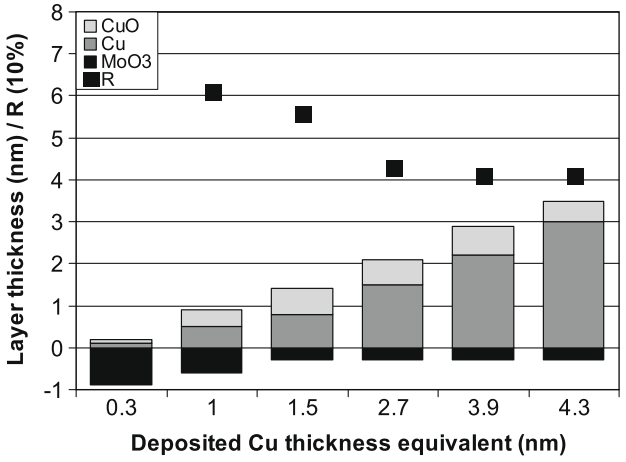


Fig. 7. Modeled ARPES results on the Cu cap, with apparent layer-by-layer growth and oxidation of Cu and Mo.

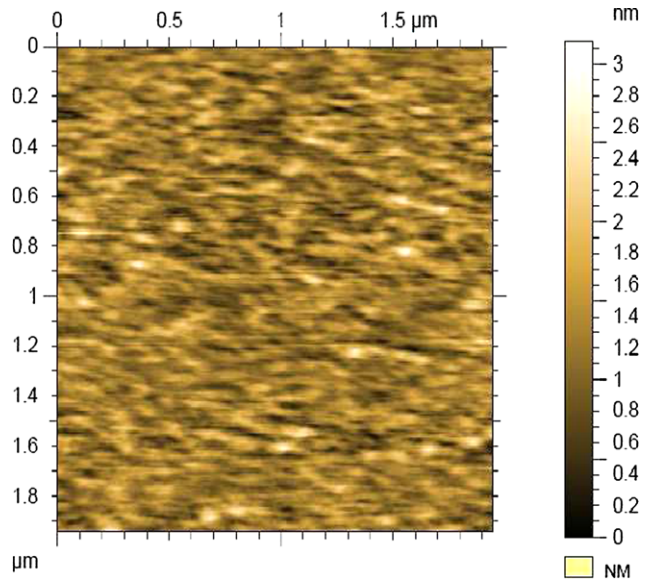


Fig. 8. AFM on a 4 nm thick Cu capping layer shows a moderate roughness compared to Au.

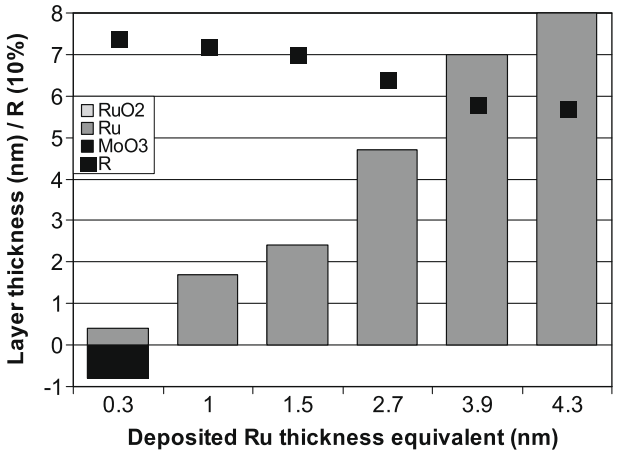


Fig. 9. Modeled ARPES results on the Ru cap, with only the 0.3 nm thick layer showing slightly increased Mo oxidation compared to bare Mo.

A Ni capping layer of 0.3 nm thickness already limits Mo oxidation to only ~15%, which is a significant reduction compared to the situations mentioned above. A 1.0 nm thick Ni capping layer further limits Mo oxidation to about 10%. Only trace amounts of MoO_3 are visible when thicker Ni layers are applied. The major part of Ni itself is oxidized up to a 0.6 nm thick Ni_2O_3 film as well as an increasing amount of NiO with deposited layer thickness. Also XPS depth profiling shows a layered Ni_2O_3/NiO/Ni/Mo structure for 1.5 nm Ni that efficiently limits subsequent Mo oxidation.

Fig. 11 shows that similar observations with ARPES are made for Co.

With a 0.3 nm thick Co cap, approximately 12% of the Mo is oxidized. For 1.0 nm thick Co this is ~7% and for thicker Co layers, virtually no Mo oxidation is observed to occur. ARPES and XPS depth profiling indicate mainly oxide presence at surface, the top monolayer bound to C, subsurface bound to Co. Co presence occurs deeper into the structure, above the Mo. The Co layer is closed and

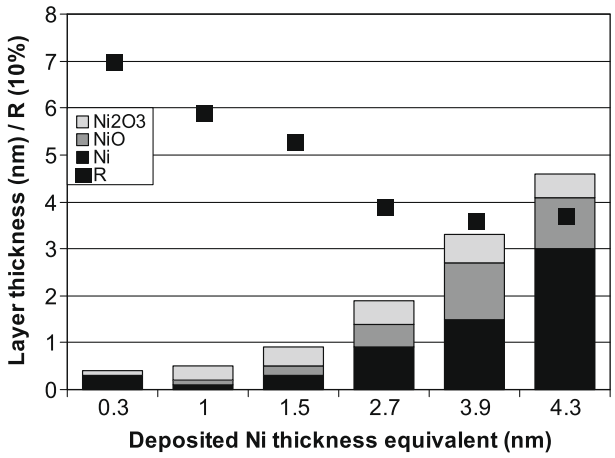


Fig. 10. Modeled ARPES results on the Ni cap, which itself is significantly oxidized but limits oxidation of Mo.

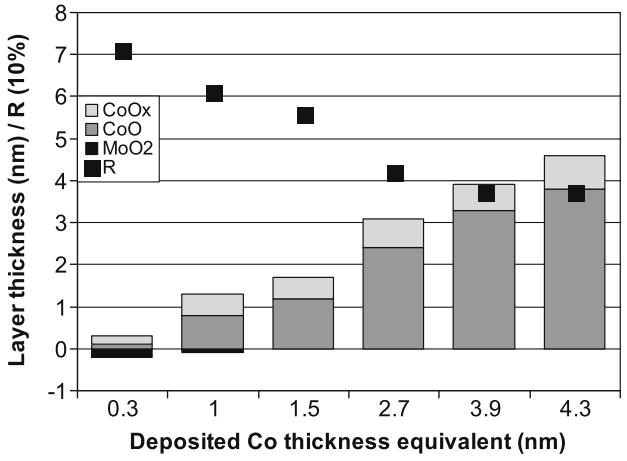


Fig. 11. Modeled ARPES results on the Co cap, completely oxidized but even more limiting Mo oxidation.

completely oxidized to CoO and on top a CoO_x film, with $x > 3$. Though heavy Co and also Ni oxidation occur and R is comparatively low, very thin layers already limit Mo oxidation under ambient conditions considerably [22], possibly by electrochemically acting as a galvanic coating [23,24].

5. Conclusions

A range of d-metal nanolayers, deposited on a Mo-on-Si substrate layer, has been studied for growth properties and protective qualities against Mo oxidation under ambient conditions as a function of nanolayer thickness. Nobler d-metal layers do oxidize less, but fail to limit Mo oxidation. These metals actually promote Mo oxidation under ambient conditions, compared to bare Mo. Significant surface roughness occurs for Cu and especially Au capped multilayers, with agglomeration in islands of typically 100 nm in diameter for Au, while Young's law predicts layer-by-layer growth. The positive $\Delta H^{\text{interface}}$ of Au with Mo appears too high a barrier for layer-by-layer growth, resulting in oxidation of exposed surface Mo to MoO_3.

Thin Pt, Pd, and Rh layers strongly promote Mo oxidation. We attribute this to creation of additional oxidation sites in the formed interlayer. The metallic Pt, Pd, and Rh generally do cover the oxidized Mo, while no subsurface oxygen is observed. Due to the more negative enthalpy for oxidation compared to the nobler metals, subsurface Mo appears to act as a sacrificial metal in an e^- donation process to support surface oxide, thus increasing its oxidation number. Rh and Ru layers of 1.0 nm and thicker grow in layer-by-layer mode on Mo and no oxidation of either metal occurs under ambient conditions. Oxidation of these catalytic capping metals is limited by on top coverage by a CO monolayer and (hydro)carbon species that absorb from the ambient and occupy absorption sites for H_2O and O_2.

With regards to surface chemistry, special interest goes to Co and Ni capping layers. ARPES modeling suggests layer-by-layer growth, as predicted by Young's law. The layers are completely oxidized and covered with large amounts of non-metallic oxide, while even single monolayers manage to largely prevent Mo oxidation. The nanolayers appear to strongly interact and involve electrochemical functioning as a galvanic coating.

Acknowledgements

This work is part of the FOM Industrial Partnership Programme I10 ('XMO') which is carried out under contract with Carl Zeiss SMT AG, Oberkochen and the 'Stichting voor Fundamenteel Onderzoek der Materie (FOM)', the latter being financially supported by the 'Nederlandse Organisatie voor Wetenschappelijk Onderzoek (NWO)'. The author wishes to thank Dr. J.G.M. van Berkum of Philips Research for the CS-EELS, HAAFD-STEM and EDX analysis.

References

[1] L.E. Klebanoff, M.E. Malinowski, P.A. Grunow, W.M. Clift, C. Steinhaus, A.H. Leung, S.J. Haney, in: Proceedings of SPIE 4343, Emerging Lithographic Technologies V, Elizabeth A. Dobisz, 2001, p. 342.
[2] N. Benoit, S. Yulin, T. Feigl, N. Kaiser, Phys. B: Condens. Matter 357 (2005) 1.
[3] E. Louis, H.-J. Voorma, N.B. Koster, L. Shmaenok, F. Bijkerk, R. Schlatmann, J. Verhoeven, Yu.Ya. Platonov, G.E. van Dorssen, H.A. Padmore, Microelectron. Eng. 23 (1994) 215.
[4] R.W.E. van de Kruijs, E. Louis, A.E. Yakshin, P. Suter, E. Zoethout, F. Bijkerk, S. Müllender, H. Enkisch, H. Trenkler, M. Wedowski, M. Weiss, B. Mertens, B. Wolschrijn, R. Jansen, A. Duisterwinkel, A. van de Runstraat, R. Klein, S. Plőger, F. Scholze, Poster 122, in: Proceedings of the Second International EUV Lithography Symposium, Antwerp, 2003.
[5] P.J. Cumpson, J. Elec. Spectros. Relat. Phenom. 73 (1995) 25.
[6] S. Tanuma, C.J. Powell, D.R. Penn, Surf. Interface Anal. 17 (1991) 911.
[7] P.C. Zalm, Surf. Interface Anal. 26 (1998) 352.
[8] J. Camarero, T. Graf, J.J. de Miguel, R. Miranda, Phys. Rev. Lett. 76 (1996) 23.
[9] T. Young, Philos. Trans. 95 (1805) 65.
[10] H. Roder, R. Schuster, K. Kern, Phys. Rev. Lett. 71 (1993) 13.
[11] M. Ohring, Material Science Thin Films; Deposition and Structure, second ed., Academic Press, San Diego, 2002.
[12] B.M. Clemens, W.D. Nix, V. Ramaswamy, J. Appl. Phys. 87 (2000) 6.
[13] F.R. de Boer, R. Boom, W.C.M. Mattens, A.R. Miedema, A.K. Niessen, Cohesion in Metals: Transition Metal Alloys, North-Holland, Amsterdam, 1988.
[14] S.H. Payne, H.J. Kreuzer, A. Pavlovska, E. Bauer, Surf. Sci. Lett. 345 (1996).
[15] T. Tsarfati, E. Zoethout, R.W.E. van de Kruijs, F. Bijkerk, submitted for publication.
[16] D. Jeon, T. Sakurai, K.D. Lee, J.W. Chung, Surf. Sci. 559 (2004).
[17] J.W. Simons, T.B. Flanagan, Can. J. Chem. 43 (1965).
[18] T. Tsarfati, E. Zoethout, R.W.E. van de Kruijs, F. Bijkerk, J. Appl. Phys. 105 (2009) 6.
[19] S. Bâjt, J. Alameda, T. Barbee, M. Clifi, J.A. Folta, B. Kauffman, E. Spiller, Soft X-Ray and Extreme Ultra-Violet Imaging Systems 11, San Diego, California, 2001.
[20] A.E. Yakshin, E. Louis, E.L.G. Maas, F. Bijkerk, R. Klein, F. Scholze, P.C. Zalm, F. Stietz, M. Wedowski, S. Muellender, B. Mertens, H. Meiling, ASET/SEMATECH Workshop on EUV Lithography, Matsue, 2001.
[21] B.M. Mertens, N. Koster, R. Jansen, A. van de Runstraat, H. Werij, F. Stietz, M. Wedowski, H. Meiling, R. Klein, R. Thornagel, F. Scholze, G. Ulm, R. Kurt, P. Zalm, E. Louis, A. Yakshin, ASET/SEMATECH Workshop on EUV Lithography, Matsue, 2001.
[22] N.S. McIntyre, D. Johnston, L.L. Coatsworth, J.R. Brown, Surf. Interface Anal. 9 (2004) 4.
[23] E. Gómez, E. Pellicer, E. Vallés, J. Electroanal. Chem. 556 (2003) 238.
[24] G.V. Kozlova, T.G. Smirnova, V.P. Molchanova, Z.A. Tubyshkina, Metal Science and Heat Treatment, vol. 4, Springer, New York, 2004. p. 7.